# Combined therapy with thrombospondin-1 type I repeats (3TSR) and chemotherapy induces regression and significantly improves survival in a preclinical model of advanced stage epithelial ovarian cancer

**Samantha Russell,* Mark Duquette,† Joyce Liu,‡ Ronny Drapkin,‡ Jack Lawler,† and Jim Petrik*,[1]**

*Department of Biomedical Sciences, University of Guelph, Guelph, Ontario, Canada; and †Beth Israel Deaconess Medical Center and ‡Dana-Farber Cancer Institute, Harvard Medical School, Boston, Massachusetts, USA

ABSTRACT **Most women are diagnosed with epithelial ovarian cancer (EOC) at advanced stage, where therapies have limited effectiveness and the long-term survival rate is low. We evaluated the effects of combined antiangiogenic and chemotherapy treatments on advanced stage EOC. Treatment of EOC cells with a recombinant version of the thrombospondin-1 type I repeats (3TSR) induced more apoptotic cell death (36.5 ± 9.6%) *in vitro* compared to untreated controls (4.1 ± 1.4). *In vivo,* tumors were induced in an orthotopic, syngeneic mouse model of advanced stage EOC. Mice were treated with 3TSR (4 mg/kg per day) alone or in combination with chemotherapy drugs delivered with maximum tolerated dose or metronomic scheduling. Pretreatment with 3TSR induced tumor regression, normalized tumor vasculature, and improved uptake of chemotherapy drugs. Combination 3TSR and metronomic chemotherapy induced the greatest tumor regression (6.2-fold reduction in size compared to PBS-treated controls) and highest survival when treatment was initiated at advanced stage. 3TSR binding to its receptor, CD36 (cluster of differentiation 36), increased binding of CD36 and SHP-1, which significantly inhibited phosphorylation of the VEGF receptor. In this study, we describe a novel treatment approach and mechanism of action with 3TSR and chemotherapy that induces regression of advanced stage EOC and significantly improves survival.—Russell, S., Duquette, M., Liu, J., Drapkin, R., Lawler, J., Petrik, J. Combined therapy with thrombospondin-1 type I repeats (3TSR) and chemotherapy induces regression and significantly improves survival in a preclinical model of advanced stage epithelial ovarian cancer. *FASEB J.* 29, 576–588 (2015). www.fasebj.org**

*Key Words:* *antiangiogenic · metronomic · vessel normalization*

OVARIAN CANCER IS THE most lethal gynecologic cancer and is the fifth leading cause of cancer-related deaths in women (1). Ovarian cancer has been termed the silent killer because the disease presents with vague, nonspecific symptoms, and women are often not diagnosed with ovarian cancer until late stage, where the 5 y survival is low (2). Typically, at diagnosis, the tumor has spread beyond the primary site and pelvic cavity, often including spread of the disease to the abdominal cavity and the formation of ascites (3). After diagnosis of epithelial ovarian cancer (EOC), women generally undergo cytoreductive surgery, followed by chemotherapeutic intervention with platinum- and taxane-based therapy. After an initial period of tumor responsiveness, chemoresistance often results, and disease progression recurs (4). As such, the development of new therapies to treat women with advanced stage ovarian cancer is essential in order to reduce the morbidity and mortality associated with this disease.

Tumors require the development of new vascular supply, through angiogenesis, to facilitate growth and metastatic spread (5), and as such, antiangiogenic strategies may provide novel therapeutic opportunities. Antiangiogenic approaches attempt to disrupt the balance between promoters and inhibitors of angiogenesis, either by inhibiting proangiogenic factors or by upregulating antiangiogenic molecules. Potent proangiogenic factors secreted by EOC cells include members of the VEGF family. Bevacizumab therapy has been tried alone and in combination in EOC clinical trials, and it has shown some promise (6). However, this approach can have severe side effects, such as hypertension, as well as rare but serious adverse effects, such as intestinal perforation (7).

Thrombospondin-1 (TSP-1) is a large extracellular matrix glycoprotein and is the first naturally occurring antiangiogenic factor described, with potent antitumor

Abbreviations: 3TSR, thrombospondin-1 type I repeats; ABAM, antibiotic/antimycotic; CD36, cluster of differentiation 36; EOC, epithelial ovarian cancer; mEC, murine microvascular endothelial cells; MET, metronomic chemotherapy; MTD, maximum tolerated dose; SHP-1, Src homology region 2 domain-containing phosphatase-1; TGF$\beta$, transforming growth factor $\beta$; TSP-1, thrombospondin-1; TSR2, second type 1 repeat of TSP-1 including amino acids 416 to 473; VEGFR-2, vascular endothelial growth factor receptor-2

[1] Correspondence: University of Guelph, 50 Stone Rd., Guelph, ON, Canada, N1G 2W1. E-mail: jpetrik@uoguelph.ca
doi: 10.1096/fj.14-261636


0892-6638/15/0029-0576 © FASEB

effects (8). The inhibitory influence of TSP-1 on tumor growth involves inhibition of angiogenesis as well as transforming growth factor $\beta$ (TGF$\beta$) activation (8, 9). Although native TSP-1 has shown antitumor and antiangiogenic effects *in vivo* in preclinical models (10), its large size and complex structure reduce its applicability as a therapeutic molecule. However, the antiangiogenic domain of TSP-1 has been predominantly localized to the 3 thrombosopondin-1 type 1 repeats, and a recombinant version of this domain, designated 3TSR, may offer promising therapeutic opportunities. The 3TSR recombinant protein has shown potent antiangiogenic and antitumor effects in an orthotopic mouse model of pancreatic cancer (11), and a single intramuscular injection of recombinant adeno-associated virus expressing 3TSR was sufficient to decrease the size and vascularity of pancreatic tumors (12).

The type 1 repeats mediate the interactions between TSP-1 and its cell surface receptors CD36 (cluster of differentiation 36) (13, 14) and integrins (15–17). Inhibition of endothelial cell migration, induction of endothelial cell apoptosis, and inhibition of the activities of proangiogenic factors have been localized primarily to 3TSR (8, 12, 17). After 3TSR binding, Fyn is recruited to CD36, and Jnk as well as caspase-3, -8, and -9 are activated, resulting in apoptotic death of endothelial cells (13, 18). CD36 activation is also known to inhibit angiogenesis through disruption of VEGF signaling by recruiting the Src homology 2 domain–containing protein tyrosine phosphatase (SHP-1) to the VEGF receptor-2 (VEGFR-2) signaling complex, and inhibiting phosphorylation of VEGFR-2 (19). The start of the second type 1 repeat contains the RFK sequence, which is responsible for activation of TGFβ (20). TGF$\beta$ activation is implicated in inhibited tumor cell proliferation and migration *in vitro* (21), and reduced tumor growth *in vivo* (22).

Two 7–amino acid type 1 repeat–based peptide mimetics, designated ABT-510 and ABT-898, have been developed for the treatment of cancer (23–26). In an orthotopic syngeneic mouse model of EOC, ABT-510- and ABT-898 induced tumor cell apoptosis (23, 27, 28) and decreased expression of VEGF, resulting in tumor vessel normalization (23, 27, 28). This vessel normalization that accompanies some forms of antiangiogenic treatment is seen as an opportunity for facilitated drug uptake and improved cancer therapy (29). We have previously shown that vascular normalization after treatment with ABT-510 and ABT-898 enhances tumor perfusion and increases tumor tissue uptake of chemotherapy drugs (23, 28). 3TSR may have antiangiogenic and antitumor advantages over these peptides because it includes all type I repeats, including the TGF$\beta$ activating domain.

Traditional chemotherapy treatment of women with ovarian cancer involves short and intermittent bursts of maximum tolerated dose (MTD) chemotherapy, which targets proliferating tumor cells (30, 31). However, recent reports have suggested that a metronomic (MET) schedule of drug delivery may be advantageous because this scheduling can have effective antitumor effects and lower total drug accumulation (32). With MET chemotherapy, drugs are delivered at a reduced dose but with increased frequency, thus reducing or eliminating the drug-free interval associated with MTD chemotherapy. In addition to effective cytotoxic effects on tumor cells, MET scheduling also has antiangiogenic effects, likely as a result of the inability of tumor vasculature to recover from the frequent administration periods (33). A significant benefit to patients is improved tolerance to MET therapy (34). Evidence suggests that combination therapy with antiangiogenic drugs and MET has excellent efficacy in a number of different cancers (35, 36), including ovarian cancer (37).

We hypothesized that 3TSR would induce vascular normalization in advanced stage EOC, which would facilitate the uptake of chemotherapy drugs delivered at low-dose MET scheduling, and that this combination therapy would induce tumor regression and significantly improve survival in patients with advanced stage EOC.

## MATERIALS AND METHODS

### Reagents and cell lines

We evaluated the effect of the 3TSR on murine and human endothelial and ovarian epithelial cells. Recombinant versions of 1) all 3 type 1 repeats of TSP-1 including amino acids 381 to 550 (3TSR), 2) the second type 1 repeat of TSP-1 including amino acids 416 to 473 (TSR2), and 3) the second type 1 repeat of TSP-1, which is extended at the amino terminal to include the TGFβ activating sequence and includes amino acids 411 to 473 (TSR2 + RFK) (22). The recombinant proteins include the vector-derived sequences RSPWG and TGHHHHHH at the N- and C-terminals, respectively, and were generated as described previously (38). Recombinant proteins that were used *in vivo* were mixed with polymyxin B–argarose (Sigma-Aldrich, St. Louis, MO, USA) for 30 min to ensure that the samples were endotoxin free ($<0.05$ EU/$\mu$g) (22).

Murine microvascular endothelial cells (mEC; ATCC, Manassas, VA, USA) were cultured in DMEM with 10% FBS, and 1% antibiotic/antimycotic (ABAM; Gibco, Grand Island, NY, USA) and HUVEC (ATCC) were cultured in F-12K supplemented with 0.1 mg/ml heparin (Sigma-Aldrich), 0.03 mg/ml endothelial cell growth supplement (Sigma-Aldrich), 10% FBS, and 1% ABAM. The following epithelial cell lines were also cultured with the appropriate media: spontaneously transformed murine ovarian surface epithelial cells (ID8 cells, generously donated by Drs. K. Roby and P. Terranova, Kansas State University, Manhattan, KS, USA; DMEM with 10% FBS and 1% ABAM); normal human ovarian surface epithelial (NOSE) cells (generously donated by Dr. J. Liu, MD Anderson Cancer Center, Houston, TX, USA); and human ovarian epithelial adenocarcinoma cell lines OVCAR-3 (ATCC; HTB-161; RPMI with 20% FBS and 1% ABAM) and SKOV3 (ATCC; HTB-77 McCoy 5A, supplemented with 10% FBS and 1% ABAM). All cell lines were immediately frozen after acquisition. Once thawed, cells were tested for morphology and growth, absence of mycoplasma was confirmed, and cells were used within 3 mo.

Primary cells were obtained from patients with advanced ovarian cancer at the Dana-Farber Cancer Institute who underwent paracentesis for malignant ascites or debulking surgery. The protocols were approved by the Dana-Farber/Harvard Cancer Center institutional review board and the Partners human research committee, and consent from patients was obtained as per institutional review board guidelines. Ascites fluid was processed, and tumor cells were purified as described previously (39). Tumor cells were grown in suspension culture in RPMI with 10% FBS, and antibiotics–antimycotics (Invitrogen, Grand Island, NY, USA).

### Mouse model

Mice were purchased from Charles River Laboratories and maintained in accordance with the Canadian Council on Animal Care. We used an orthotopic, syngeneic mouse model of EOC as described previously (15). Briefly, transformed murine ovarian surface epithelial cells from C57BL6 mice (ID8; $1.0 \times 10^6$) were injected directly under the ovarian bursa of syngeneic mice. In this model, 60 d after tumor induction, mice form primary ovarian masses, and by 80 d after tumor induction, there are large ovarian tumors, numerous secondary peritoneal lesions, and abdominal ascites, which replicates the clinical profile of women with stage III EOC (40)—the disease stage that the majority of women are diagnosed with (41). To determine the ability of 3TSR to induce regression of established EOC, tumors were allowed to develop for 60 or 80 d after tumor induction, at which time treatment was initiated with intraperitoneal once-daily injections of 3TSR (4 mg/kg) or D5W vehicle control (200 $\mu$l). 3TSR has not shown any toxicity or immune response in this syngeneic mouse model. Mice were killed 100 d after tumor induction, which corresponded to 20 d of treatment. Primary tumors were collected, and peritoneal tumors were assessed for metastatic spread on the basis of a lesion scoring system, as previously reported (23, 27, 28, 42).

### Immunoblotting and coimmunoprecipitation

Murine and human cancer and endothelial cells were lysed and subjected to Western blot analysis, as previously reported (23, 27). Membranes were probed for overnight at 4°C for VEGF (1:600 dilution; Santa Cruz Biotechnology, Burlingame, CA, USA), VEGFR-2 (1:500 dilution; Santa Cruz Biotechnology), phospho-VEGR-2 (1:500; detects tyrosine 1175; Abcam, Cambridge, United Kingdom); FasL (1:600; Pharmingen, Franklin Lakes, NY, USA), cleaved caspase-3 (1:1000 dilution; Abcam), bcl-2 (1:500; Santa Cruz Biotechnology), CD36 (1:600 dilution; Pharmingen), SHP-1 (1:1000 dilution; Abcam), or Fyn (1:1000 dilution; BD Transduction Laboratories, San Jose, CA, USA). Antibody expression was visualized with Western Lightning Chemiluminescence Reagent Plus (PerkinElmer BioSignal Inc., Montreal, QC, Canada). Computer-assisted densitometry was performed by AlphaEase FC software (AlphaInnotech, San Leandro, CA, USA), and results were quantified and reported as integrated densitometry values relative to $\beta$-actin or tubulin. For coimmunoprecipitation experiments, ID8 cells remained untreated or were treated with 10 nM 3TSR for 24 h, trypsinized and washed, lysed, and protein collected as above. The cell lysate was immediately used for immunoprecipitation experiments. To preclear the samples, 1 ml of cell lysate, 5 $\mu$g nonimmune IgG, and 25 $\mu$l protein G agarose beads were mixed for 1 h at 4°C. After removal of the protein G beads by centrifugation, 5 $\mu$g of anti-CD36 (Pharmingen) was added and the samples incubated for 3 h at 4°C. Then 25 $\mu$l of protein G beads were added and the samples incubated for an additional 3 h at 4°C. The beads were then washed 3 times in lysis buffer, and the precipitated complex was eluted in 50 $\mu$l of boiling 2× SDS-PAGE loading buffer for 4 min. The samples were separated by SDS-PAGE and transferred to nitrocellulose membrane, which was incubated in 5% skim milk in Tris-buffered saline–Tween-20 (TBST) for 1 h, followed by incubation with primary anti-SHP-1 (1:1000 dilution; Abcam) overnight at 4°C.

### Immunofluorescence

After treatment on glass coverslips, cells were fixed in 10% neutral buffered formalin for 1 h at room temperature and rinsed in PBS. Tissues were fixed overnight in 10% formalin, then washed for 24 h in 70% ethanol and rinsed in PBS before embedding, sectioning (5 $\mu$m), and mounting on glass slides. Cells were permeabilized by adding 0.1% Triton X-100 (Sigma-Aldrich) for 15 min at room temperature, blocked for 10 min in 5% BSA in PBS, and exposed to primary antibodies: anti-active caspase-3 (1:200 dilution; Abcam), anti-Ki67 (1:200; Abcam), anti-FasL (1:200; Pharmingen), anti-CD36 (1:400; Pharmingen), anti–phospho-VEGFR-2, (1:500; Abcam, recognizes tyrosine 1175), or anti-SHP-1 (1:600; Abcam) overnight at 4°C. AlexaFluor-conjugated secondary antibodies (1:100; Invitrogen) were added for 2 h at room temperature, followed by incubation with DAPI (Sigma-Aldrich) for 10 min. Cells were imaged with an Olympus inverted epifluorescence microscope and Metamorph integrated morphometry software.

### Cell death and proliferation

To determine changes in the incidence of tumor cell death and proliferation during ovarian tumor development, tumors were collected at 30, 60, and 90 d after tumor induction from mice treated with daily 200 $\mu$l intraperitoneal injections of PBS or 3TSR (4 mg/kg per day). Tumors were fixed in 10% neutral buffered formalin and subjected to TUNEL (terminal deoxynucleotidyl transferase dUTP nick end labeling) analysis according the manufacturer's instructions (Roche, Basel, Switzerland) to determine the percentage of apoptotic tumor cells. Tumors were also immunostained with an anti-Ki67 antibody (1:200; Abcam) to quantify the percentage of proliferating tumor cells.

### Antiangiogenic and chemotherapy treatments

We evaluated the effect of combined antiangiogenic and chemotherapy therapies on the treatment of advanced stage EOC. EOC was induced by the injection of $1 \times 10^6$ ID8 cells as described above. Tumors were allowed to grow for 60 d without intervention to allow the mice to develop ovarian cancer symptoms that replicate women with stage III EOC, with large primary tumors, numerous metastatic abdominal lesions, and the accumulation of abdominal ascites (40). At 60 d after tumor induction, mice began daily intraperitoneal injections of PBS (200 $\mu$l) or 3TSR (4 mg/kg per day in 200 $\mu$l PBS). These treatments continued for 14 d to allow for potential 3TSR-mediated tumor cell apoptosis and tumor vessel normalization. At this point (74 d after tumor induction), mice were organized into the following groups: PBS alone (control), 3TSR (4 mg/kg per day), MTD (10 mg/kg carboplatin/10 mg/kg paclitaxel twice a week); MET (2 mg/kg carboplatin/1 mg/kg paclitaxel 4 times a week); 3TSR + MTD; and 3TSR + MET. Mice continued treatment until 90 d after tumor induction, when they were euthanized, tumors collected, and mice scored for the number of metastatic tumors present as well as the presence of ascites. At euthanasia, tumors were weighed and measured to determine changes in tumor weight and size, respectively.

### Vessel density and maturity

Tumors were collected from PBS- and 3TSR-treated mice at 30, 60, and 90 d after tumor induction and subjected to immunofluorescence colocalization in which tissues were stained with anti-CD31 antibody (1:50; Abcam) to detect vascular endothelial cells and anti–smooth muscle actin antibody (1:400; Santa Cruz Biotechnology) to identify vascular pericytes. Changes in blood vessel density were also quantified after *in vivo* antiangiogenic and chemotherapy treatments, as described above. Endothelial

cells in tissues collected at 90 d after tumor induction were immunolocalized with an anti-CD31 antibody (1:50; Cell Signaling Technology, Danvers, MA, USA). Blood vessel density was reported as the percentage of tissue comprising CD31 plus blood vessels in each treatment group ($n = 6$ mice/group).

### Tissue hypoxia and drug uptake

At 90 d after tumor induction, tumor tissue collected from PBS- and 3TSR- (4 mg/kg per day) treated mice were immunostained with an anti–carbonic anhydrase antibody (1:500; Abcam) to indicate tissue hypoxia. Image capture and analysis was performed using bright-field microscopy to determine the percentage of carbonic anhydrase–positive, hypoxic tumor tissue. To determine changes in drug uptake, a second group of PBS- or 3TSR-treated (4 mg/kg per day) mice at 90 d after tumor induction ($n = 3$/group) were injected with (40 $\mu$Ci) tritiated paclitaxel (Moravek Biochemicals and Radiochemicals, Brea, CA, USA) intraperitoneally. Twelve, 24, or 48 h after injection, mice were killed; primary tumors were collected and homogenized in scintillation fluid, and tissue isotope uptake was measured via scintillation counting in a Tricarb liquid scintillation counter (PerkinElmer, Waltham, MA, USA).

### Survival

In a second cohort of mice, daily treatments with 3TSR were initiated at 60 or 80 d after tumor induction (12 animals per group), and animals continued to receive treatment until they became moribund, which was assessed on the basis of noticeable ascites and an increased weight gain of 20% of their pretumor induction body weight. All animals were killed at 150 d after tumor induction, and data from those that were free of morbidity (*i.e.,* had not developed ascites fluid) were recorded accordingly. The ovaries of these animals were assessed histologically to ensure that the surgical injection of ID8 cells was successful and created the presence of a focal necrotic region from which regressed tumors had originated.

### Statistical analysis

For determination of statistical significance for experiments with immunohistochemistry, Western blot analysis, and tumor morphology, 2-way ANOVA was performed, followed by *post hoc* analysis with Tukey's test. For evaluation of survival after antiangiogenic and chemotherapy treatments, the log-rank test was performed by GraphPad Prism v6 software (GraphPad Software, La Jolla, CA). Unless stated otherwise, statistical significance was considered at $P < 0.05$.

## RESULTS

### 3TSR induces cell death in ovarian cancer cells *in vitro*

ID8s were subjected to increasing dosages of 3TSR *in vitro,* and cells were assessed for their expression of apoptotic and survival factors. 3TSR significantly increased expression of the apoptotic marker cleaved caspase-3 at concentrations as low as 1 $\mu$mol (**Fig. 1*A***). This increase in apoptosis was correlated with increased expression of proapoptotic FasL and decreased expression of the survival factor VEGF, as well as the cytoprotective proto-oncogene bcl-2 (Fig. 1*A*). Because VEGF signaling is known to confer survival in these cells (23, 27, 42), they were treated in the presence or absence of VEGF (to activate VEGFR-2) or 3TSR (to antagonize this cytoprotective effect). 3TSR significantly reduced VEGF-induced phosphorylation and activation of VEGFR-2 (Fig. 1*B*). Treatment of ID8 cells with 5 $\mu$mol 3TSR showed a significant ($P < 0.01$) increase in TUNEL-positive cells and a converse significant ($P < 0.05$) decrease in ID8 cell proliferation; these changes were associated with increased cell expression of FasL (Fig. 1*C*).

### Specific type I repeat effects on ovarian cancer cell apoptosis and proliferation

CD36 has been reported to mediate the inhibitory effects of the TSP-1 type 1 repeat region on endothelial cells and angiogenesis (8, 43). In addition, knockdown of CD36 decreases the ability of ABT-510 to inhibit EOC cell proliferation and induce apoptosis (27). Similarly, knockdown of CD36 diminishes the activity of 3TSR to inhibit proliferation and induce apoptosis of ID8 cells (**Fig. 2**). The knockdown cells displayed a 75% to 80% decrease in CD36 (data not shown). Thus, the residual activity of 3TSR seen in ID8 cells with decreased CD36 may reflect this partial knockdown. Alternatively, other receptors for 3TSR, such as $\beta$1 integrins, may participate, either alone or in combination with CD36, to support 3TSR binding. The results indicate that the majority of activity seen with 3TSR compounds is mediated by CD36.

The 28-2 cell line was prepared by isolating cells from the ascites of ID8 tumor-bearing mice (42). These cells grow more rapidly than the parental ID8 cell *in vitro* and *in vivo* (42). They also express increased levels of VEGF, phospho-VEGFR-2, p-Akt, and bcl-2, and decreased amounts of Bax compared to ID8 cells (42). We observed that 3TSR was equally as effective in inhibiting proliferation and inducing apoptosis of 28-2 cells as it was for ID8 cells (Fig. 2). These data indicate that 3TSR effectively targets aggressive EOC cells that have acquired the ability to propagate in the peritoneal cavity and are associated with late stage disease.

To establish that the effect of 3TSR on EOC cell proliferation and apoptosis was not specific to ID8 cells, we treated 2 human cell lines, OVCAR-3 and SKOV-3, with 3TSR. As shown in Fig. 2, treatment of these human cell lines with 3TSR at the concentration that is effective for ID8 and 28-2 cells (10 nM) produced a significant decrease in proliferation and increase in apoptosis in all cell lines compared to serum-free controls.

Inhibition of B16F10 melanoma growth by 3TSR is partially mediated by activation of TGF$\beta$ (22). The amino acid sequence (RFK) required for TGF$\beta$ activation by 3TSR lies between the first and second TSRs, designated TSR1 and TSR2, respectively. We have prepared recombinant versions of TSR2 that include the RFK sequence (TSR2 + RFK) or do not include it (TSR2) to probe the role of TGF$\beta$ activation by TSP-1 in the tumor microenvironment (22). In these experiments, we first titrated the response to recombinant proteins for 3TSR, TSR2, and TSR2 + RFK (Fig. 2). 3TSR and TSR2 + RFK exhibit activity as low as 10 pM concentrations (Fig. 2). Maximal

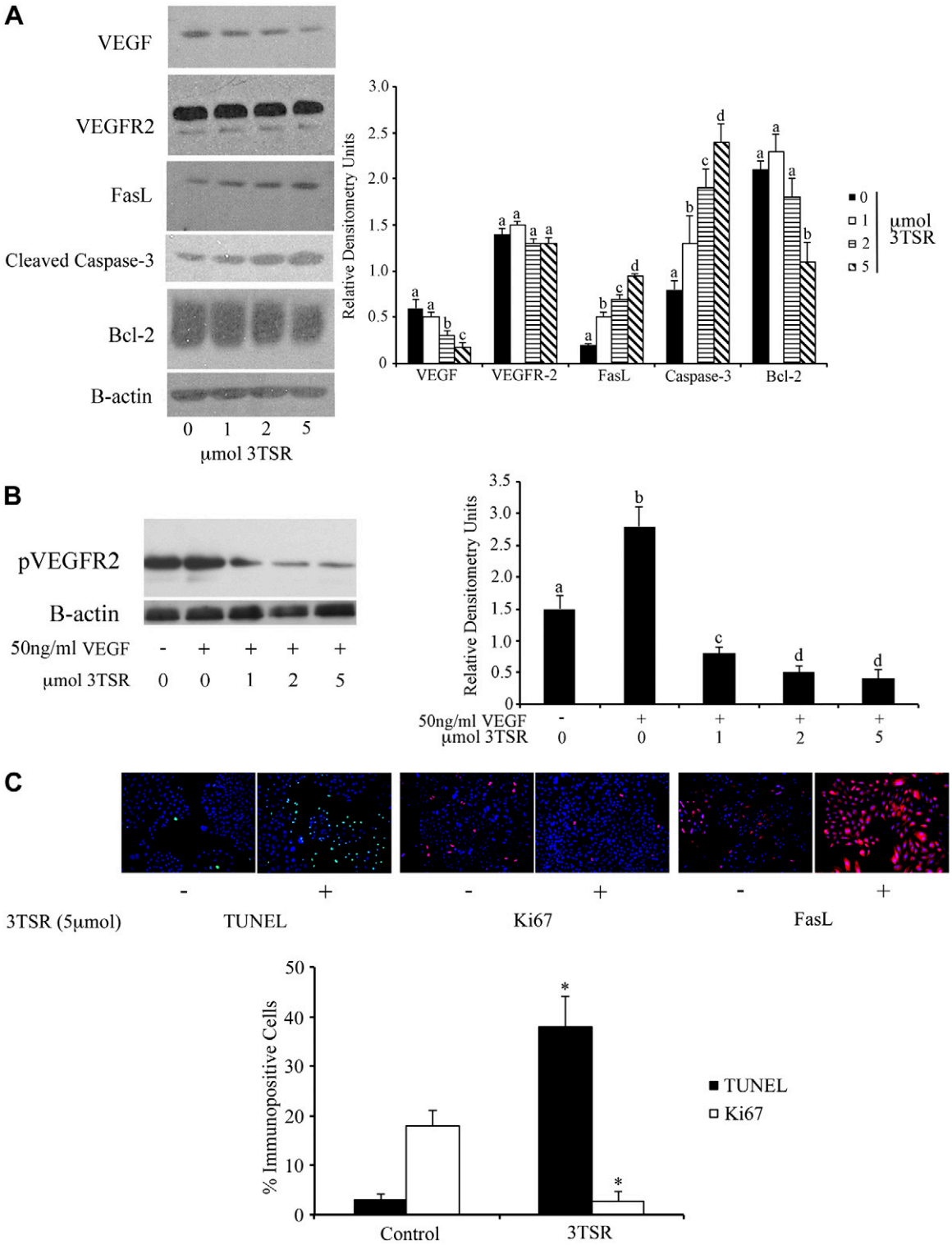


**Figure 1.** 3TSR treatment of ID8 cells *in vitro* affects gene expression. Spontaneously transformed murine ovarian cancer cells (ID8) were treated with varying concentrations of 3TSR for 24 h. *A*) 3TSR treatment increased the expression of proapoptotic proteins and decreased expression of the survival factor bcl-2. *B*) 3TSR treatment decreased expression of phosphorylated VEGFR-2. Bars with different letters are statistically different ($P < 0.05$) within each antibody group. *C*) ID8 cells were treated in the presence or absence of 5 $\mu$mol 3TSR for 24 h and subjected to TUNEL analysis or immunofluorescence for Ki67 or FasL. 3TSR treatment increased the proportion of TUNEL- and FasL-positive cells while decreasing the percentage of Ki67-positive proliferating cells compared to untreated controls. *Statistically different ($P < 0.05$) compared to controls.

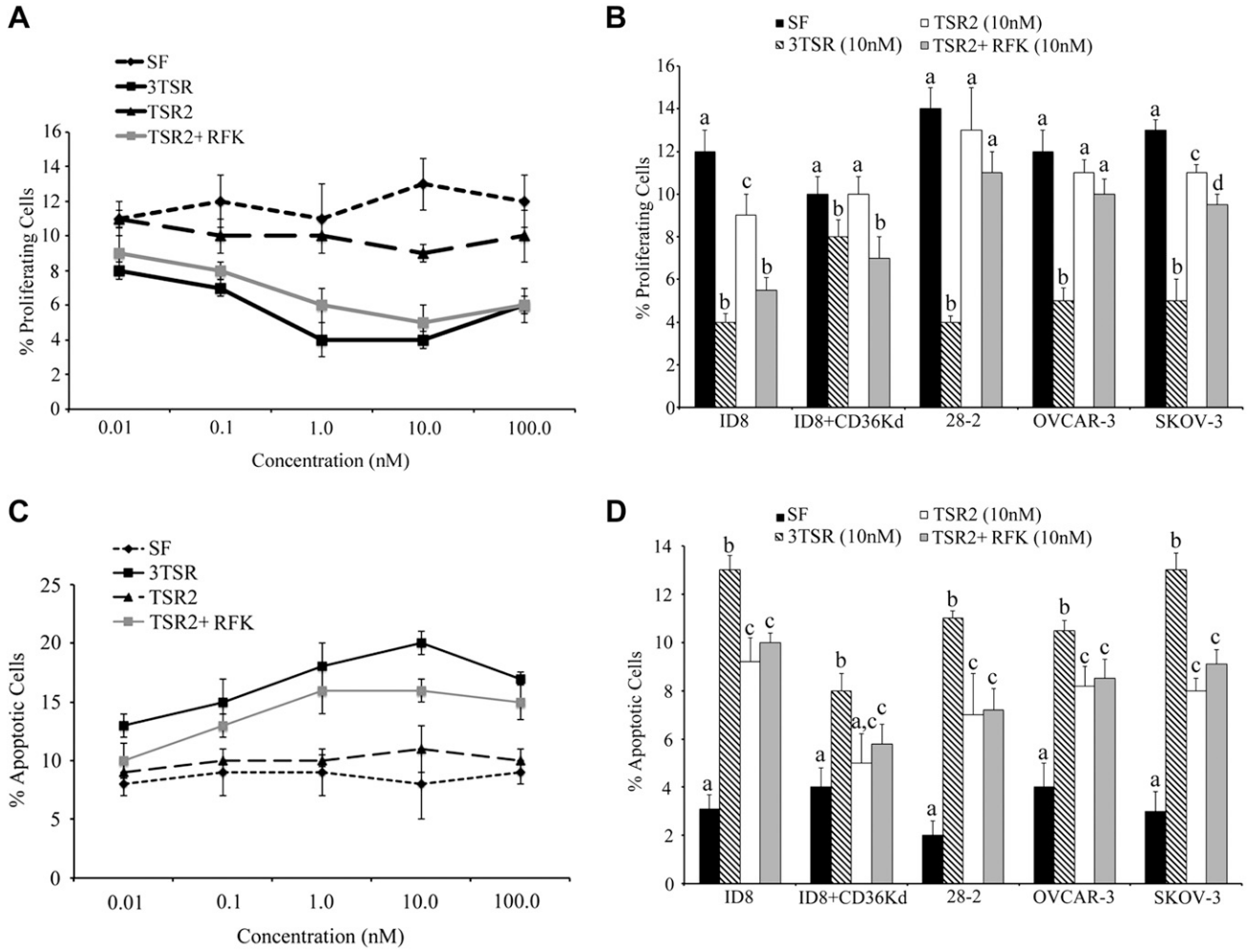


**Figure 2.** 3TSR alters cell proliferation and death predominantly through CD36-dependent mechanisms. Murine ID8 cells were cultured in the absence or presence of increasing concentrations of 3TSR, TSR2, and TSR2 + RFK for 24 h and analyzed for changes in proliferation and apoptosis. Intact ID8 cells and ID8 CD36 knockdown (KD) cells, reprogrammed metastatic murine ovarian cancer cells (28-2), and human ovarian cancer cells (OVCAR-3, SKOV-3) were treated with 10 nM 3TSR, TSR2, or TSR2 + RFK for 24 h and analyzed for changes in proliferation and apoptosis. *A*) Serum-free and TSR2 treatment did not alter ID8 cell proliferation Conversely, 3TSR and TSR2 + RFK decreased proliferation. *B*) When compared to serum-free controls and TSR2 and TSR2 + RFK treatments, 3TSR reduced cell proliferation in all ovarian cancer cell types tested, except for CD36KD. *C*) Serum-free and TSR2 treatment had no effect on ID8 cell apoptosis, while 3TSR and TSR2 + RFK increased the incidence of cell death. *D*) 3TSR treatment resulted in the highest increase in ovarian cancer cell apoptosis in all cell lines tested, while with both TSR2 and TSR2 + RFK increased apoptosis compared to serum-free controls, but no changes in the incidence of apoptosis were seen between the 2 groups. For the bar graphs, columns with different letters are statistically different ($P < 0.05$) within each cell type.

inhibition of ID8 cell proliferation and induction of apoptosis were observed between 1 and 10 nM for 3TSR and TSR2 + RFK. TSR2 + RFK had a greater inhibitory effect on EOC cell proliferation than TSR2 alone, although the effect was not as great as that seen after 3TSR treatment (Fig. 2). TSR2 and TSR2 + RFK showed a similar induction of apoptosis, which was greater than serum-free treatment but less than the apoptosis induced by 3TSR (Fig. 2).

### 3TSR induces changes in tumor cell survival, blood vessel morphometry, and tissue perfusion *in vivo*

Tumor tissue was collected from mice treated with PBS or 3TSR (4 mg/kg per day) at 30, 60, and 90 d after tumor induction and subjected to TUNEL analysis and immunostaining for Ki67 to quantify changes in apoptosis and proliferation, respectively. 3TSR induced a significant ($P < 0.05$) increase in tumor cell apoptosis at all time points (**Fig. 3*A***) and a significant ($P < 0.05$) decrease in tumor cell proliferation at 60 and 90 d after tumor induction (Fig. 3*A*). Tumor tissue was also probed for changes in tumor vasculature. Immunofluorescence colocalization showed an increase in the proportion of mature, pericyte-covered blood vessels in the 3TSR-treated group at 30, 60, and 90 d after tumor induction compared to the PBS-treated controls (Fig. 3*B*). Quantification of the total number of CD31-positive blood vessels per field of view revealed a significant ($P < 0.05$) decrease in vessel density in 3TSR tumors at 60 and 90 d after tumor induction compared to PBS-treated control tumors (Fig. 3*B*). Carbonic anhydrase immunohistochemistry to indirectly measure

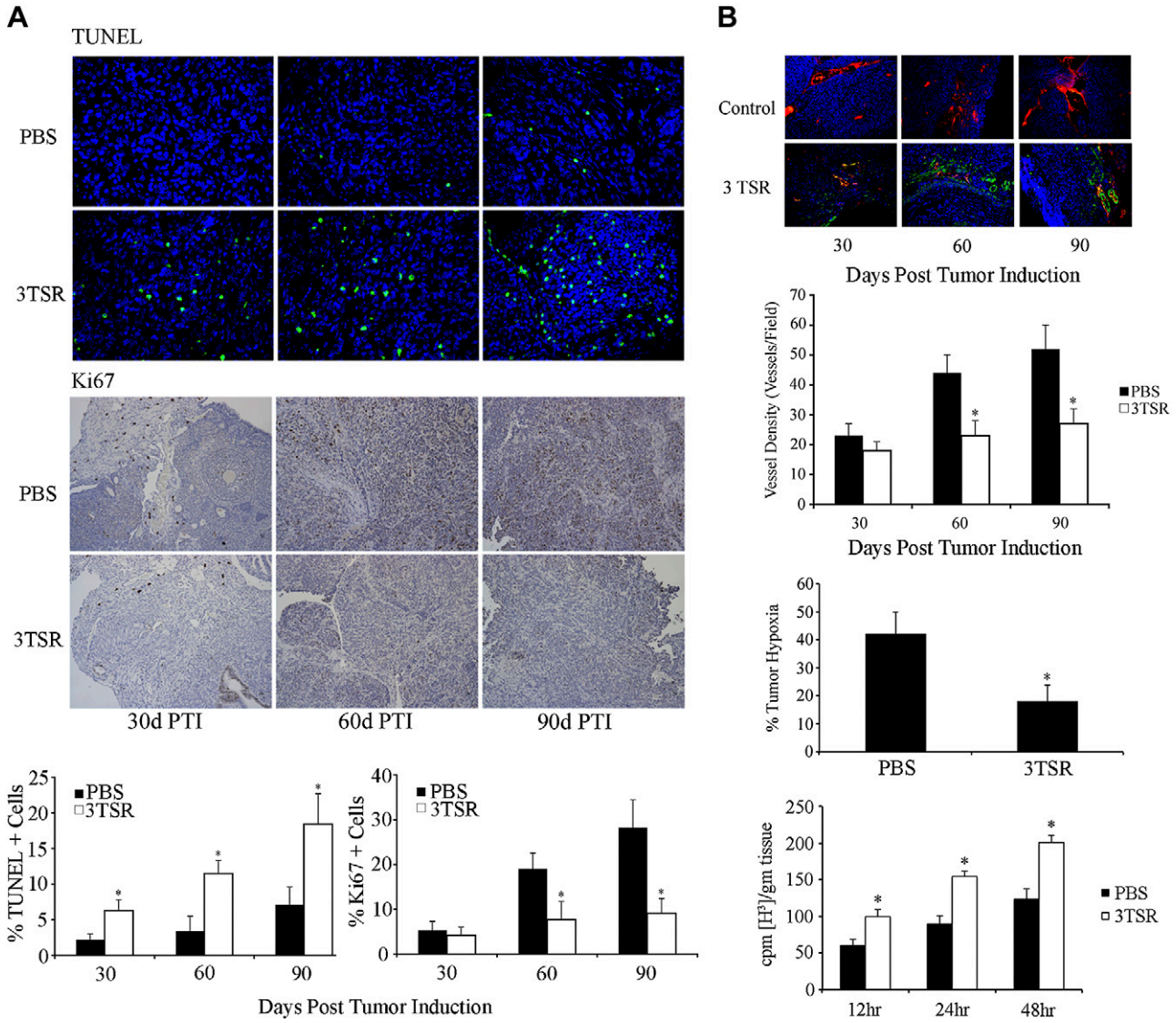


**Figure 3.** 3TSR induces tumor cell apoptosis and decreases tumor cell proliferation. *A*) 3TSR treatment was initiated at the time of tumor induction, and tumors were collected 30, 60, and 90 d later. 3TSR-treated mice had significantly (*$P < 0.05$) higher incidence of tumor cell apoptosis and reduced rates of tumor cell proliferation. At 30 d after tumor induction, normal ovary is evident, as are newly developing tumors. At 60 and 90 d after tumor induction, images represent tumor tissue exclusively. *B*) 3TSR treatment induces vascular normalization, facilitates tumor perfusion, and increases chemotherapy drug uptake. Immunofluorescence colocalization of endothelial cell (CD31, red) and pericyte ($\alpha$ smooth muscle actin, green) showed an increased proportion of mature, pericyte-covered blood vessels in 3TSR-treated tumors compared to controls. 3TSR treatment significantly ($P < 0.05$) reduced tumor vessel density compared to controls at 60 and 90 d after tumor induction. There was reduced tumor tissue hypoxia in 90 d tumors treated with 3TSR compared to controls. Mice at 90 d after tumor induction were injected with tritiated paclitaxel. Tumors were then excised 12, 24, and 48 h after injection, and isotope uptake was measured. 3TSR-treated tumors had a significant ($P < 0.01$) increase in tissue uptake of the radiolabeled chemotherapy drug.

hypoxia was performed on 90 d after tumor induction tissue from 3TSR- and PBS-treated mice. 3TSR treatment resulted in a significant ($P < 0.05$) decrease in the percentage hypoxic tumor tissue compared to PBS-treated controls. To determine whether enhanced tissue perfusion would improve drug uptake, at 90 d after tumor induction, PBS- and 3TSR-treated mice were injected with tritiated paclitaxel (40 $\mu$Ci) intraperitoneally, and tissues were homogenized and subjected to scintillation counting 12, 24, and 48 h after collection. The 3TSR treatment significantly ($P < 0.05$) increased radioisotope uptake compared to PBS-treated controls.

### 3TSR treatment induces tumor and disease regression when initiated at advanced stages of disease

When disease in mice was allowed to progress without intervention for 80 d after tumor induction, the animals developed late stage III disease with large primary tumors, numerous metastatic peritoneal lesions, and abdominal ascites. When treatment was initiated at 80 d after tumor induction, by 100 d after tumor induction, PBS-treated mice had tumors that had grown to almost twice the size ($P < 0.05$) of the tumor size at the initiation of treatment (**Fig. 4*A***). Conversely, by 100 d after tumor induction,

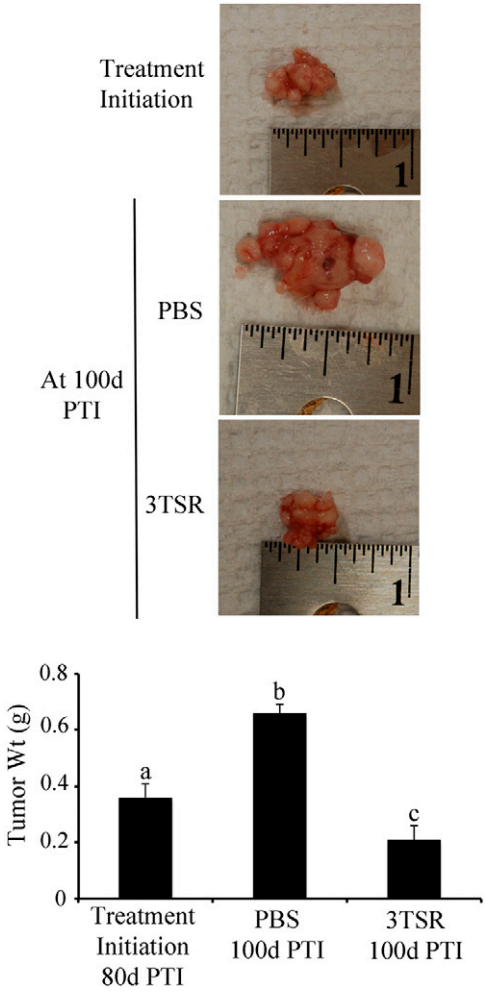


**Figure 4.** 3TSR induces regression of advanced stage ovarian cancer. *A*) Mice were injected with $1 \times 10^6$ ID8 cells under the ovarian bursa, and tumors were allowed to develop without intervention until 80 d after tumor induction. At this point, the mice exhibited signs similar to those seen in women with stage III ovarian cancer. At 80 d after tumor induction, mice either received daily PBS injection or 4 mg/kg 3TSR i.p. for 20 d, at which time the mice were euthanized and the tumors removed. Representative tumor (top) demonstrating the size of tumors at the time of treatment initiation (80 d after tumor induction). After 20 d of treatment, PBS-treated control tumors were significantly larger, whereas 3TSR tumors were significantly smaller than the tumors at 80 d after tumor induction, indicating that not only was tumor growth inhibited but also that tumor regression was induced. Bars with different letters are statistically different ($P < 0.05$). *B*) 3TSR significantly reduces morbidity at 100 d after tumor induction compared to PBS-treated controls. In 3TSR-treated mice, none exhibited abdominal ascites compared to all PBS controls. Five of 6 mice had complete absence of abdominal metastatic tumors, while the majority of PBS-treated controls had more than 10 metastatic tumors.

3TSR treatment induced tumor regression, and tumors were significantly ($P < 0.05$) smaller in volume and lighter in weight than the tumors at the initiation of treatment (Fig. 4*A*). At 100 d after tumor induction, mice were assessed for signs of disease morbidity, and the number of peritoneal lesions and number of mice with ascites were quantified. All of the PBS-treated mice had ascites, and all had a minimum of 3 metastatic peritoneal lesions (Fig. 4*B*). 3TSR treatment resulted in an absence of abdominal ascites in any of the mice, and all but one mouse had elimination of metastatic disease (Fig. 4*B*).

### Combination antiangiogenic and MET significantly induces disease regression and improves survival *in vivo*

After tumor initiation in mice, the disease was allowed to progress without intervention for 60 d after tumor induction, at which time the mice exhibited disease characteristics similar to women with stage III EOC, with large primary tumors, metastatic abdominal disease, and the beginning of ascites accumulation. Treatment was initiated at this time to determine whether combined antiangiogenic and chemotherapy treatment would be effective in advanced stage disease. At 60 d after tumor induction, mice were either treated with PBS or 3TSR (4 mg/kg per day) for 14 d to initiate vessel normalization. At 74 d after tumor induction, mice either received PBS or 3TSR alone or in combination with chemotherapy drugs delivered with MTD or MET scheduling until 100 d after tumor induction. All treatments significantly ($P < 0.001$) reduced tumor size compared to PBS-treated controls (**Fig. 5*A***). Combination 3TSR and MET chemotherapy resulted in a further significant ($P < 0.05$) reduction in tumor size compared to all other treatments (Fig. 5*A*). Tissues collected at 100 d after tumor induction were immunostained with an anti-CD31 antibody to visualize and quantify tumor blood vessels. The 3TSR, MET, and 3TSR + MTD treatments significantly ($P < 0.05$) reduced tumor vessel density compared to PBS-treated controls (Fig. 5*B*). Combined 3TSR and MET therapy resulted in a further significant ($P < 0.05$) reduction in tumor vessel density (Fig. 5*B*). In a second cohort of mice, the treatment protocol was repeated, but the disease was allowed to progress until mice exhibited signs of clinical morbidity, including abdominal distension due to ascites and weight gain greater than 20% of their original weight. MTD and MET therapies conferred a significant survival advantage compared to PBS-treated controls (Fig. 5*C*), while 3TSR and 3TSR + MTD treatments prolonged survival compared to PBS and either chemotherapy drug alone (Fig. 5*C*). Combination 3TSR + MET therapy conferred the most significant survival advantage compared to all other treatments (Fig. 5*C*).

### Primary tumor cells express CD36

We used patient-derived ovarian cancer cells to determine the expression of various proteins that have been reported to be involved in the response of endothelial cells to TSP-1 and/or 3TSR. All cell preparations ($n = 8$) tested expressed readily detectable levels of CD36 (**Fig. 6*A***). In endothelial cells, the interaction of 3TSR with CD36 results in the activation of Fyn to induce apoptosis and the recruitment of SHP-1 to suppress signaling through the VEGF prosurvival pathway (19). SHP-1 was detected in all 8 of the cell preparations tested, and Fyn was present in 7 of the 8 (Fig. 6*A*). VEGF was also detected

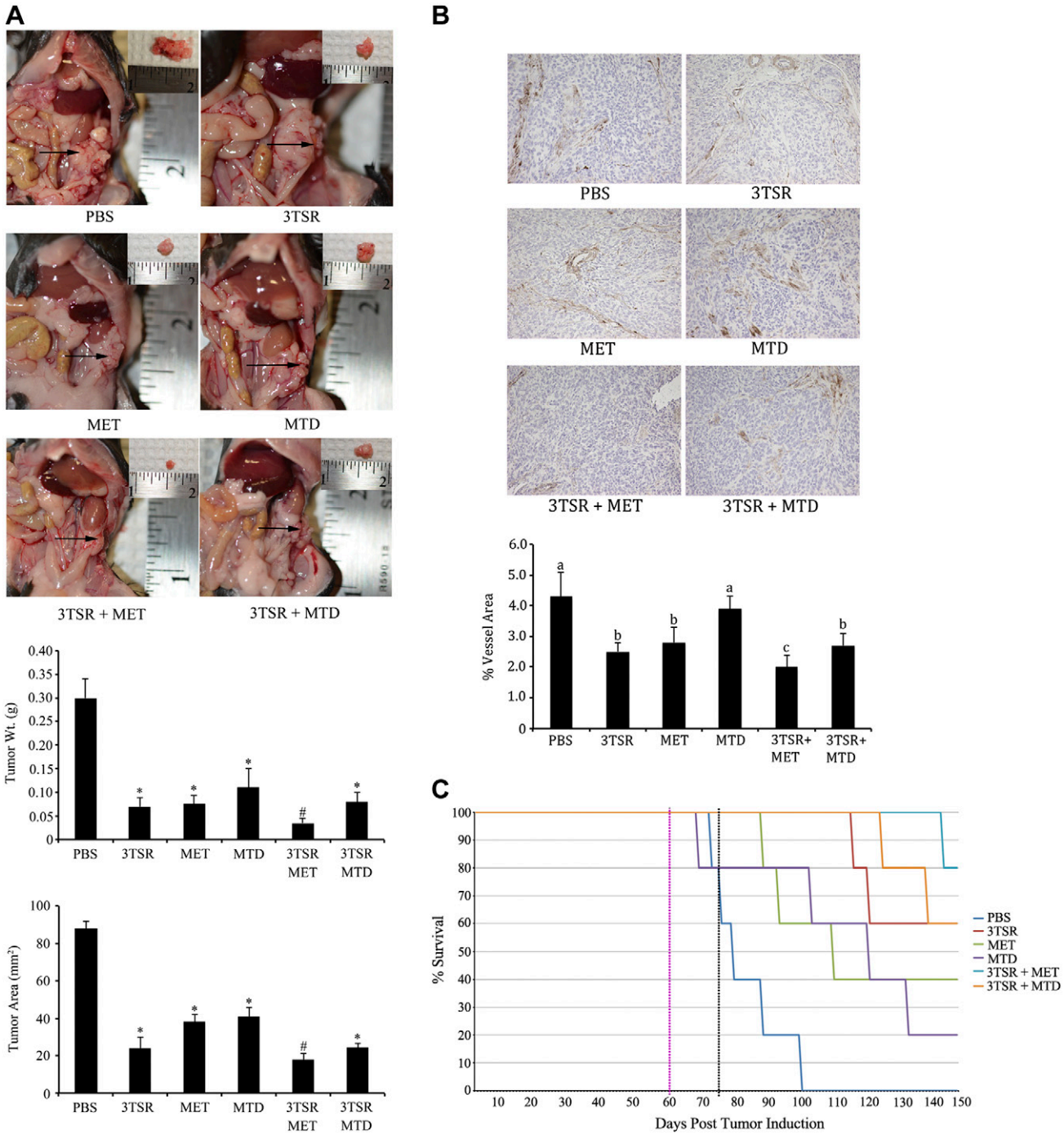


**Figure 5.** Combined treatment with 3TSR and MET induces regression of advanced stage ovarian cancer. *A*) At stage III ovarian cancer, mice began a 20 d treatment regimen with 3TSR and chemotherapy delivered with traditional MTD or low-dose MET chemotherapy drug scheduling. All treatments significantly ($P < 0.05$) reduced tumor weight compared to PBS-treated controls. Combined therapy with 3TSR and MET induced significant ($P < 0.05$) tumor regression compared to all other treatment regimens, with a 6.2-fold reduction in tumor size compared to PBS-treated controls. For the bar graphs, treatment groups with different symbols are statistically different ($P < 0.05$). Primary tumors *in situ* are indicated by the black arrow. *B*) Tumor blood vessel density after 3TSR treatment alone or in combination with chemotherapy drugs administered with MTD or MET scheduling. 3TSR and MET treatments significantly ($P < 0.05$) reduced tumor vessel density, with 3TSR/MET combination therapy having the largest ($P < 0.05$) reduction in tumor vascularity. Blood vessels are indicated by CD31-positive brown stain against the hematoxylin background. For the bar graph, bars with different letters are statistically different ($P < 0.05$). *C*) 3TSR and MET chemotherapy treatment initiated at advanced stage disease improves disease-free survival. Tumors were induced in mice and allowed to progress to stage III disease without intervention. Mice were then treated with 3TSR and chemotherapy drugs administered with MTD or MET scheduling alone or in combination. Log-rank analysis showed that 3TSR and MET combination therapy significantly ($P < 0.05$) improved survival compared to all other therapies. Log-rank analysis also showed that the presence of 3TSR significantly ($P < 0.05$) improved survival compared to untreated controls and to the MTD and MET chemotherapies administered individually.

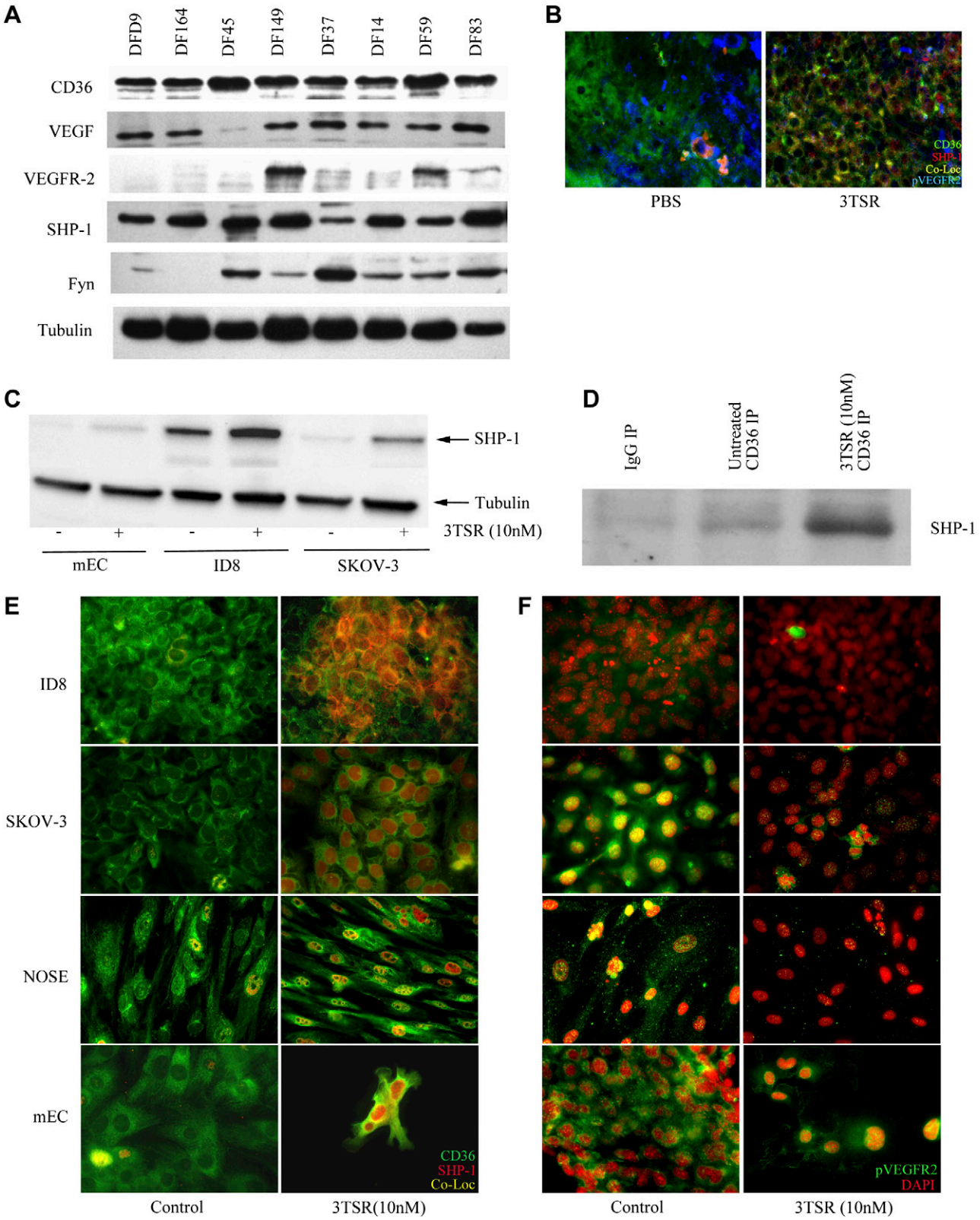


**Figure 6.** Protein expression of ovarian cancer cells in the presence and absence of 3TSR. *A*) Protein extracts of cells isolated from the ascites of ovarian cancer patients were blotted for the presence of proteins (indicated on the left) that have been reported to mediate the response of endothelial cells to TSP-1 and/or 3TSR. Immunoblotting for tubulin was used as a control for protein loading. *B*) Tumor tissue collected at 90 d after tumor induction from mice treated with PBS or 3TSR (4 mg/kg per day) was immunostained for CD36 (green), SHP-1 (red), and phospho-VEGFR-2 (blue). *C*) mEC, murine (ID8), and human (SKOV-3) EOC cells were cultured for 24 h in the presence or absence of 3TSR (10 nM), and Western blot analysis was performed for SHP-1. The 3TSR treatment resulted in an increase in SHP-1 protein expression. *D*) Coimmunoprecipitation was

(*continued on next page*)

in all 8 of the cell extracts; however, the expression in one cell preparation (DF45) was markedly lower than the others. VEGFR-2 was also detected in all of the cell extracts; however, in most of them, it appeared as multiple bands, suggesting that a portion of the protein was being taken up and degraded in the continuous presence of VEGF (44, 45). We were unable to detect TSP-1 in these cells by Western blot analysis, which may be indicative of the protective, pro-VEGF environment created by these cells. Triple immunofluorescence colocalization was performed on tumors from PBS- and 3TSR-treated mice at 90 d after tumor induction in order to evaluate protein colocalization between CD36 and SHP-1 and whether this interaction was associated with changes in expression of phosphorylated VEGFR-2. Treatment with 3TSR resulted in colocalization of CD36 and SHP-1 and decreased tissue expression of VEGFR-2 phosphorylated on tyrosine 1175 (Fig. 6*B*). The 3TSR treatment of microvascular endothelial cells and murine (ID8) and human (SKOV-3) EOC cells resulted in an increase in expression of SHP-1 protein (Fig. 6*C*). Coimmunoprecipitation experiments showed low levels of binding between CD36 and SHP-1 in untreated conditions, but when cells were stimulated with 10 nM 3TSR for 24 h, there was an increase in the amount of SHP-1 protein bound to CD36 (Fig. 6*D*). When endothelial, EOC, and NOSE cells were treated with 3TSR, there was an increase in expression of SHP-1 expression and colocalization with CD36 compared to control cells, which appeared to express CD36 but very low levels of SHP-1 (Fig. 6*E*). Immunofluorescence staining revealed a decrease in expression of phospho-VEGFR-2 in endothelial, ovarian epithelial, and EOC cells after treatment with 3TSR *in vitro* (Fig. 6*F*).

## DISCUSSION

In this study, we have identified a new and highly effective therapeutic approach to the treatment of EOC that combines 3TSR with MET. The majority of mice treated in this way display a durable response, as indicated by dramatic increases in survival and little evidence of disease at the time of euthanasia. In an effort to closely model human disease and increase the likelihood that the results will translate to the clinic, we have: 1) used an orthotopic model so that the primary tumors and metastases grow in the appropriate microenvironment, 2) implanted the ID8 cells into syngeneic immune competent C57BL/6 mice, 3) delivered the treatment as an intervention trial after the disease progressed to stage III, and 4) used survival as one of the end points.

In this model, 3TSR as a single agent is more efficacious than MTD chemotherapy with carboplatin and paclitaxel. This strong activity may result from the fact that 3TSR targets multiple aspects of ovarian cancer (**Fig. 7**). In addition to directly inhibiting angiogenesis, 3TSR

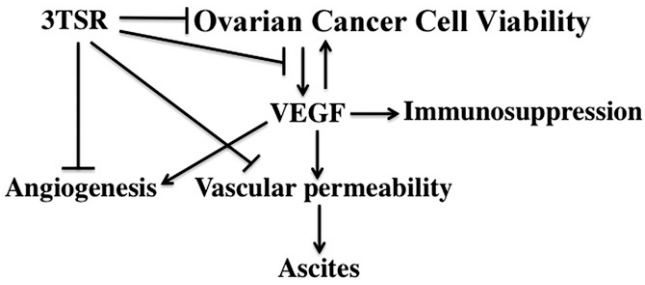


**Figure 7.** Schematic representation of the effects of 3TSR on EOC. 3TSR has direct effects on the growth and survival of both the ovarian cancer cells and endothelial cells. In addition, 3TSR suppresses VEGF production by EOC cells, leading to decreased autocrine growth signaling, increased immunosuppression, and decreased ascites. 3TSR may also inhibit vascular permeability through inhibition of VEGF signal transduction.

inhibits proliferation and induces apoptosis of EOC cells. To our knowledge, this is the first time that a direct effect of 3TSR on tumor cells has been observed. Knockdown of CD36 suppresses the effect of 3TSR on EOC cell proliferation and apoptosis, suggesting a similar role for 3TSR and CD36 that is seen in endothelial cells (13). 3TSR also suppresses the production of VEGF by EOC cells, which would result in a further decrease in angiogenesis, decrease in EOC cell survival, decrease in ascites production, and decrease in immunosuppression (46–48). 3TSR has also been shown to inhibit VEGF-induced vascular permeability in the Miles assay, raising the possibility that 3TSR suppresses ascites production (14).

The data presented here and in previous studies indicate that 3TSR is considerably more effective than ABT-898 in promoting survival in the ID8 model of ovarian cancer (23). Multiple peptides in the type 1 repeats of TSP-1, including some that do not overlap with the ABT-510 and ABT-898 sequence, have antiangiogenic activity (49, 50). The structure of the type 1 repeats indicates that they fold in such a way that the various antiangiogenic peptides come together to form a single motif (51). It is not possible for a 7–amino acid peptide to mimic the full structure and function of the type 1 repeats. Our data indicate the 3TSR is also more active than a single correctly folded type 1 repeat, and we thus have chosen to use the 3TSR recombinant protein to capture their full activity.

The combination of 3TSR with MET was found to be particularly effective for the treatment of EOC. MET has been shown to increase Fas expression by tumor cells, and 3TSR up-regulates FasL on endothelial cells (52, 53). The addition of MET to ABT-510 results in greater inhibition of angiogenesis and tumor growth (52, 53). In the current study, we have observed that 3TSR increases FasL on EOC cells. We hypothesize that homotypic and heterotypic cell-to-cell interactions among Fas and FasL on EOC

performed after treatment for 24 h with 3TSR, pulling down with anti-CD36 antibody and probing for SHP-1 by Western blot analysis. 3TSR treatment increased coexpression of CD36 and SHP-1. *E*) mEC, ID8, SKOV-3, and normal NOSE cells were cultured for 24 h in the presence or absence of 3TSR (10 nM), and immunofluorescence labeling was performed for CD36 (green) and SHP-1 (red). 3TSR treatment resulted in increased expression of SHP-1 and colocalization with CD36. *F*) Expression of phospho-VEGFR-2 was measured in ID8, SKOV-3, NOSE, and mEC cells with or without 3TSR treatment.

and that endothelial cells promote apoptosis in the 3TSR/MET combination therapy. It is also worth noting that MET has been reported to increase systemic endogenous TSP-1 expression, which may further contribute to the inhibitory activity observed here (33).

The effects of 3TSR on EOC proliferation and apoptosis may in part be mediated by suppression of phosphorylation of VEGFR-2. VEGF has been reported to act as an autocrine factor for EOC cells by activating VEGFR-2 (46, 47). The 3TSR-induced decrease in VEGF synthesis would be expected to down-regulate this signal transduction pathway. In addition, we have observed that 3TSR increases the expression of SHP-1, a phosphatase that has been shown to mediate suppression of VEGFR-2 phosphorylation by TSP-1 in endothelial cells (19). Thus, 3TSR induces changes in protein levels that act to suppress the activity of the VEGF signal transduction pathway. TSP-1 can also inhibit tumor growth through activation of TGF$\beta$ if the tumor cells retain the ability to respond to TGF$\beta$ (22). Our comparison of recombinant proteins that possess or lack the TGF$\beta$ activating sequence suggest that active TGF$\beta$ suppresses the growth of ID8 cells, but not OVCAR-3 or SKOV-3 cells. Because we did not add exogenous TGF$\beta$ in these experiments, the different responses my reflect differences in endogenous TGF$\beta$ expression. With respect to tumor cell apoptosis, 3TSR induced more cell death than either of the two TSR2-containing recombinant proteins for all cells lines tested, implying that the inclusion of all 3 TSRs is necessary for optimal activity. This conclusion is consistent with reports that peptide sequences within the first and third TSRs have inhibitory activity in angiogenesis assays (54). The data imply that activation of TGF$\beta$ is not required for 3TSR activity against EOC cells *in vitro*.

Effective and minimally toxic treatments for EOC represent an important unmet need in clinical oncology. In this study, we have shown that 3TSR recombinant protein targets multiple aspects of EOC progression and has considerable potential for the treatment of EOC as a single agent or when combined with MET. It may also be effective to combine 3TSR with VEGF pathway antagonists to reduce the dose and thus the adverse effects associated with these drugs. A recent phase I study has reported that a combination of ABT-510 and bevacizumab is well tolerated and may be clinically useful for treatment of solid tumors (55). Future studies will determine whether increasing the exposure of 3TSR though continuous drug delivery devices or through incorporation into Fc fusion proteins increases the activity of 3TSR. Such approaches may expedite translation of 3TSR into the clinic. FJ

The authors appreciate the technical assistance of M. Ross, K. Osz, J. Curtis, and H. Piao. This work was supported by grants from the Canadian Institutes for Health Research (450084) and Ovarian Cancer Canada to J.P., and U.S. National Institutes of Health National Cancer Institute Grant CA130895 and NIH National Institute of Neurological Disorders and Stroke Grant NS077797 and CAO Pilot Grant from Beth Israel Deaconess Medical Center to J.L.

## REFERENCES

1. Siegel, R., Ma, J., Zou, Z., and Jemal, A. (2014) Cancer statistics, 2014. *CA Cancer J. Clin.* **64**:252–271
2. Longuespée, R., Boyon, C., Desmons, A., Vinatier, D., Leblanc, E., Farré, I., Wisztorski, M., Ly, K., D'Anjou, F., Day, R., Fournier, I., and Salzet, M. (2012) Ovarian cancer molecular pathology. *Cancer Metastasis Rev.* **31**, 713–732
3. Vaughan, S., Coward, J. I., Bast, R. C., Jr., Berchuck, A., Berek, J. S., Brenton, J. D., Coukos, G., Crum, C. C., Drapkin, R., Etemadmoghadam, D., Friedlander, M., Gabra, H., Kaye, S. B., Lord, C. J., Lengyel, E., Levine, D. A., McNeish, I. A., Menon, U., Mills, G. B., Nephew, K. P., Oza, A. M., Sood, A. K., Stronach, E. A., Walczak, H., Bowtell, D. D., and Balkwill, F. R. (2011) Rethinking ovarian cancer: recommendations for improving outcomes. *Nat. Rev. Cancer* **11**, 719–725
4. Galluzzi, L., Senovilla, L., Vitale, I., Michels, J., Martins, I., Kepp, O., Castedo, M., and Kroemer, G. (2012) Molecular mechanisms of cisplatin resistance. *Oncogene* **31**, 1869–1883
5. Folkman, J. (1971) Tumor angiogenesis: therapeutic implications. *N. Engl. J. Med.* **285**, 1182–1186
6. Zhou, M., Yu, P., Qu, X., Liu, Y., and Zhang, J. (2013) Phase III trials of standard chemotherapy with or without bevacizumab for ovarian cancer: a meta-analysis. *PLoS ONE* **8**, e81858
7. Borofsky, S. E., Levine, M. S., Rubesin, S. E., Tanyi, J. L., Chu, C. S., and Lev-Toaff, A. S. (2013) Bevacizumab-induced perforation of the gastrointestinal tract: clinical and radiographic findings in 11 patients. *Abdom. Imaging* **38**, 265–272
8. Lawler, J., and Detmar, M. (2004) Tumor progression: the effects of thrombospondin-1 and -2. *Int. J. Biochem. Cell Biol.* **36**, 1038–1045
9. Zhang, J., Yang, W., Zhao, D., Han, Y., Liu, B., Zhao, H., Wang, H., Zhang, Q., and Xu, G. (2014) Correlation between TSP-1, TGF-beta and PPAR-gamma expression levels and glioma microvascular density. Oncol. Lett. **7**, 95–100
10. Allegrini, G., Goulette, F. A., Darnowski, J. W., and Calabresi, P. (2004) Thrombospondin-1 plus irinotecan: a novel antiangiogenic-chemotherapeutic combination that inhibits the growth of advanced human colon tumor xenografts in mice. *Cancer Chemother. Pharmacol.* **53**, 261–266
11. Zhang, X., Galardi, E., Duquette, M., Delic, M., Lawler, J., and Parangi, S. (2005) Antiangiogenic treatment with the three thrombospondin-1 type 1 repeats recombinant protein in an orthotopic human pancreatic cancer model. *Clin. Cancer Res.* **11**, 2337–2344
12. Zhang, X., Xu, J., Lawler, J., Terwilliger, E., and Parangi, S. (2007) Adeno-associated virus–mediated antiangiogenic gene therapy with thrombospondin-1 type 1 repeats and endostatin. *Clin. Cancer Res.* **13**, 3968–3976
13. Ren, B., Song, K., Parangi, S., Jin, T., Ye, M., Humphreys, R., Duquette, M., Zhang, X., Benhaga, N., Lawler, J., and Khosravi-Far, R. (2009) A double hit to kill tumor and endothelial cells by TRAIL and antiangiogenic 3TSR. *Cancer Res.* **69**, 3856–3865
14. Zhang, X., Kazerounian, S., Duquette, M., Perruzzi, C., Nagy, J. A., Dvorak, H. F., Parangi, S., and Lawler, J. (2009) Thrombospondin-1 modulates vascular endothelial growth factor activity at the receptor level. *FASEB J.* **23**, 3368–3376
15. Lawler, J., and Hynes, R. O. (1989) An integrin receptor on normal and thrombasthenic platelets that binds thrombospondin. *Blood* **74**, 2022–2027
16. Calzada, M. J., Annis, D. S., Zeng, B., Marcinkiewicz, C., Banas, B., Lawler, J., Mosher, D. F., and Roberts, D. D. (2004) Identification of novel beta1 integrin binding sites in the type 1 and type 2 repeats of thrombospondin-1. *J. Biol. Chem.* **279**, 41734–41743
17. Short, S. M., Derrien, A., Narsimhan, R. P., Lawler, J., Ingber, D. E., and Zetter, B. R. (2005) Inhibition of endothelial cell migration by thrombospondin-1 type-1 repeats is mediated by beta1 integrins. *J. Cell Biol.* **168**, 643–653
18. Jiménez, B., Volpert, O. V., Crawford, S. E., Febbraio, M., Silverstein, R. L., and Bouck, N. (2000) Signals leading to apoptosis-dependent inhibition of neovascularization by thrombospondin-1. *Nat. Med.* **6**, 41–48
19. Chu, L. Y., Ramakrishnan, D. P., and Silverstein, R. L. (2013) Thrombospondin-1 modulates VEGF signaling via CD36 by recruiting SHP-1 to VEGFR2 complex in microvascular endothelial cells. *Blood* **122**, 1822–1832
20. Crawford, S. E., Stellmach, V., Murphy-Ullrich, J. E., Ribeiro, S. M., Lawler, J., Hynes, R. O., Boivin, G. P., and Bouck, N. (1998) Thrombospondin-1 is a major activator of TGF-beta1 in vivo. *Cell* **93**, 1159–1170
21. Pierce, D. F., Jr., Gorska, A. E., Chytil, A., Meise, K. S., Page, D. L., Coffey, R. J., Jr., and Moses, H. L. (1995) Mammary tumor

suppression by transforming growth factor beta 1 transgene expression. *Proc. Natl. Acad. Sci. USA* **92**, 4254–4258
22. Miao, W. M., Seng, W. L., Duquette, M., Lawler, P., Laus, C., and Lawler, J. (2001) Thrombospondin-1 type 1 repeat recombinant proteins inhibit tumor growth through transforming growth factor-beta-dependent and -independent mechanisms. *Cancer Res.* **61**, 7830–7839
23. Campbell, N., Greenaway, J., Henkin, J., and Petrik, J. (2011) ABT-898 induces tumor regression and prolongs survival in a mouse model of epithelial ovarian cancer. *Mol. Cancer Ther.* **10**, 1876–1885
24. Gordon, M. S., Mendelson, D., Carr, R., Knight, R. A., Humerickhouse, R. A., Iannone, M., and Stopeck, A. T. (2008) A phase 1 trial of 2 dose schedules of ABT-510, an anti-angiogenic, thrombospondin-1-mimetic peptide, in patients with advanced cancer. *Cancer* **113**, 3420–3429
25. Recouvreux, M. V., Camilletti, M. A., Rifkin, D. B., Becu-Villalobos, D., and Díaz-Torga, G. (2012) Thrombospondin-1 (TSP-1) analogs ABT-510 and ABT-898 inhibit prolactinoma growth and recover active pituitary transforming growth factor-$\beta$1 (TGF-$\beta$1). *Endocrinology* **153**, 3861–3871
26. Sahora, A. I., Rusk, A. W., Henkin, J., McKeegan, E. M., Shi, Y., and Khanna, C. (2012) Prospective study of thrombospondin-1 mimetic peptides, ABT-510 and ABT-898, in dogs with soft tissue sarcoma. *J. Vet. Intern. Med.* **26**, 1169–1176
27. Greenaway, J., Henkin, J., Lawler, J., Moorehead, R., and Petrik, J. (2009) ABT-510 induces tumor cell apoptosis and inhibits ovarian tumor growth in an orthotopic, syngeneic model of epithelial ovarian cancer. *Mol. Cancer Ther.* **8**, 64–74
28. Campbell, N. E., Greenaway, J., Henkin, J., Moorehead, R. A., and Petrik, J. (2010) The thrombospondin-1 mimetic ABT-510 increases the uptake and effectiveness of cisplatin and paclitaxel in a mouse model of epithelial ovarian cancer. *Neoplasia* **12**, 275–283
29. Carmeliet, P., and Jain, R. K. (2011) Principles and mechanisms of vessel normalization for cancer and other angiogenic diseases. *Nat. Rev. Drug Discov.* **10**, 417–427
30. Harries, M., and Gore, M. (2002) Part II: chemotherapy for epithelial ovarian cancer-treatment of recurrent disease. *Lancet Oncol.* **3**, 537–545
31. Harries, M., and Gore, M. (2002) Part I: chemotherapy for epithelial ovarian cancer-treatment at first diagnosis. *Lancet Oncol.* **3**, 529–536
32. Gately, S., and Kerbel, R. (2001) Antiangiogenic scheduling of lower dose cancer chemotherapy. *Cancer J.* **7**, 427–436
33. Bocci, G., Fioravanti, A., Orlandi, P., Di Desidero, T., Natale, G., Fanelli, G., Viacava, P., Naccarato, A. G., Francia, G., and Danesi, R. (2012) Metronomic ceramide analogs inhibit angiogenesis in pancreatic cancer through up-regulation of caveolin-1 and thrombospondin-1 and down-regulation of cyclin D1. *Neoplasia* **14**, 833–845
34. Scharovsky, O. G., Mainetti, L. E., and Rozados, V. R. (2009) Metronomic chemotherapy: changing the paradigm that more is better. *Curr. Oncol.* **16**, 7–15
35. Mayer, E. L., Isakoff, S. J., Klement, G., Downing, S. R., Chen, W. Y., Hannagan, K., Gelman, R., Winer, E. P., and Burstein, H. J. (2012) Combination antiangiogenic therapy in advanced breast cancer: a phase 1 trial of vandetanib, a VEGFR inhibitor, and metronomic chemotherapy, with correlative platelet proteomics. *Breast Cancer Res. Treat.* **136**, 169–178
36. Kelley, R. K., Hwang, J., Magbanua, M. J., Watt, L., Beumer, J. H., Christner, S. M., Baruchel, S., Wu, B., Fong, L., Yeh, B. M., Moore, A. P., Ko, A. H., Korn, W. M., Rajpal, S., Park, J. W., Tempero, M. A., Venook, A. P., and Bergsland, E. K. (2013) A phase 1 trial of imatinib, bevacizumab, and metronomic cyclophosphamide in advanced colorectal cancer. *Br. J. Cancer* **109**, 1725–1734
37. Kamat, A. A., Kim, T. J., Landen, C. N., Jr., Lu, C., Han, L. Y., Lin, Y. G., Merritt, W. M., Thaker, P. H., Gershenson, D. M., Bischoff, F. Z., Heymach, J. V., Jaffe, R. B., Coleman, R. L., and Sood, A. K. (2007) Metronomic chemotherapy enhances the efficacy of antivascular therapy in ovarian cancer. *Cancer Res.* **67**, 281–288
38. Yee, K. O., Streit, M., Hawighorst, T., Detmar, M., and Lawler, J. (2004) Expression of the type-1 repeats of thrombospondin-1 inhibits tumor growth through activation of transforming growth factor-beta. *Am. J. Pathol.* **165**, 541–552
39. Clauss, A., Ng, V., Liu, J., Piao, H., Russo, M., Vena, N., Sheng, Q., Hirsch, M. S., Bonome, T., Matulonis, U., Ligon, A. H., Birrer, M. J., and Drapkin, R. (2010) Overexpression of elafin in ovarian carcinoma is driven by genomic gains and activation of the nuclear factor kappaB pathway and is associated with poor overall survival. *Neoplasia* **12**, 161–172
40. Li, L., Wang, L., Zhang, W., Tang, B., Zhang, J., Song, H., Yao, D., Tang, Y., Chen, X., Yang, Z., Wang, G., Li, X., Zhao, J., Ding, H., Reed, E., and Li, Q. Q. (2004) Correlation of serum VEGF levels with clinical stage, therapy efficacy, tumor metastasis and patient survival in ovarian cancer. *Anticancer Res.* **24**(3b), 1973–1979
41. Berkenblit, A., and Cannistra, S. A. (2005) Advances in the management of epithelial ovarian cancer. *J. Reprod. Med.* **50**, 426–438
42. Greenaway, J., Moorehead, R., Shaw, P., and Petrik, J. (2008) Epithelial–stromal interaction increases cell proliferation, survival and tumorigenicity in a mouse model of human epithelial ovarian cancer. *Gynecol. Oncol.* **108**, 385–394
43. Dawson, D. W., Pearce, S. F., Zhong, R., Silverstein, R. L., Frazier, W. A., and Bouck, N. P. (1997) CD36 mediates the *in vitro* inhibitory effects of thrombospondin-1 on endothelial cells. *J. Cell Biol.* **138**, 707–717
44. Horowitz, A., and Seerapu, H. R. (2012) Regulation of VEGF signaling by membrane traffic. *Cell. Signal.* **24**, 1810–1820
45. Simons, M. (2012) An inside view: VEGF receptor trafficking and signaling. *Physiology (Bethesda)* **27**, 213–222
46. Sher, I., Adham, S. A., Petrik, J., and Coomber, B. L. (2009) Autocrine VEGF-A/KDR loop protects epithelial ovarian carcinoma cells from anoikis. *Int. J. Cancer* **124**, 553–561
47. Adamcic, U., Skowronski, K., Peters, C., Morrison, J., and Coomber, B. L. (2012) The effect of bevacizumab on human malignant melanoma cells with functional VEGF/VEGFR2 autocrine and intracrine signaling loops. *Neoplasia* **14**, 612–623
48. Yigit, R., Massuger, L. F., Figdor, C. G., and Torensma, R. (2010) Ovarian cancer creates a suppressive microenvironment to escape immune elimination. *Gynecol. Oncol.* **117**, 366–372
49. Dawson, D. W., Volpert, O. V., Pearce, S. F., Schneider, A. J., Silverstein, R. L., Henkin, J., and Bouck, N. P. (1999) Three distinct D–amino acid substitutions confer potent antiangiogenic activity on an inactive peptide derived from a thrombospondin-1 type 1 repeat. *Mol. Pharmacol.* **55**, 332–338
50. Iruela-Arispe, M. L., Lombardo, M., Krutzsch, H. C., Lawler, J., and Roberts, D. D. (1999) Inhibition of angiogenesis by thrombospondin-1 is mediated by 2 independent regions within the type 1 repeats. *Circulation* **100**, 1423–1431
51. Tan, K., Duquette, M., Liu, J. H., Dong, Y., Zhang, R., Joachimiak, A., Lawler, J., and Wang, J. H. (2002) Crystal structure of the TSP-1 type 1 repeats: a novel layered fold and its biological implication. *J. Cell Biol.* **159**, 373–382
52. Quesada, A. J., Nelius, T., Yap, R., Zaichuk, T. A., Alfranca, A., Filleur, S., Volpert, O. V., and Redondo, J. M. (2005) In vivo upregulation of CD95 and CD95L causes synergistic inhibition of angiogenesis by TSP1 peptide and metronomic doxorubicin treatment. *Cell Death Differ.* **12**, 649–658
53. Yap, R., Veliceasa, D., Emmenegger, U., Kerbel, R. S., McKay, L. M., Henkin, J., and Volpert, O. V. (2005) Metronomic low-dose chemotherapy boosts CD95-dependent antiangiogenic effect of the thrombospondin peptide ABT-510: a complementation antiangiogenic strategy. *Clin. Cancer Res.* **11**, 6678–6685
54. Tolsma, S. S., Volpert, O. V., Good, D. J., Frazier, W. A., Polverini, P. J., and Bouck, N. (1993) Peptides derived from two separate domains of the matrix protein thrombospondin-1 have antiangiogenic activity. *J. Cell Biol.* **122**, 497–511
55. Uronis, H. E., Cushman, S. M., Bendell, J. C., Blobe, G. C., Morse, M. A., Nixon, A. B., Dellinger, A., Starr, M. D., Li, H., Meadows, K., Gockerman, J., Pang, H., and Hurwitz, H. I. (2013) A phase I study of ABT-510 plus bevacizumab in advanced solid tumors. *Cancer Med.* **2**, 316–324

*Received for publication August 7, 2014.*
*Accepted for publication September 23, 2014.*